THE JOURNAL OF PHYSICAL CHEMISTRY B

Article

pubs.acs.org/JPCB

Co-Grafting of Amino–Poly(ethylene glycol) and Magainin I on a TiO_2 Surface: Tests of Antifouling and Antibacterial Activities

Jessie Peyre,[†] Vincent Humblot,[†] Christophe Méthivier,[†] Jean-Marc Berjeaud,[§] and Claire-Marie Pradier*[,†]

[†]CNRS UMR 7197, Surface Reactivity Laboratory, Pierre et Marie Curie University - Paris 6, 3 rue Galilée 94200 Ivry-sur-Seine, France

[§]Ecology & Biology Interactions - UMR 7267 CNRS, Poitiers University, IBMIG, 40 avenue du recteur Pineau, 86022 Poitiers Cedex, France

Supporting Information

ABSTRACT: An antimicrobial peptide,[1] Magainin I (Mag), was grafted to a titanium oxide surface, via an antiadhesive poly(ethylene glycol) (PEG) cross-linker. The latter plays a 2-fold part, being antiadhesive, and enabling the covalent immobilization of the peptide. The functionalization was characterized at each step by reflection absorption infrared spectroscopy (RAIRS) and X-ray photoelectron spectroscopy (XPS). The antiadhesive properties of PEG, and antibacterial activity of the anchored Magainin I, were individually tested toward adsorption of bovin serum albumin (BSA) proteins, and against Gram positive bacteria, *Listeria ivanovii*, respectively. The results reveal that adhesion of both proteins and bacteria have been considerably reduced, accompanied by an inhibition of the growth of remaining adhered bacteria. This work thus offers a novel approach to functionalize oxide surfaces against biofilms and to measure the so-obtained properties in each of the successive steps of a biofilm formation.

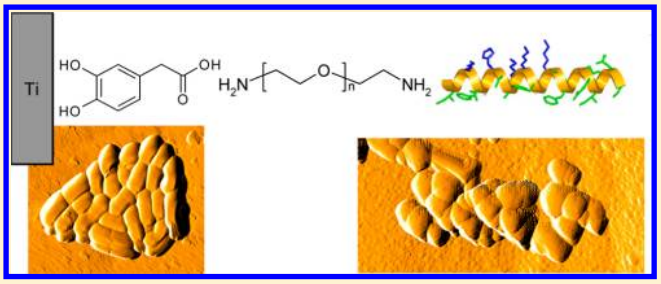

INTRODUCTION

In any biological environment, microorganisms have a strong tendency to adhere and grow on solid surfaces. Once bacteria or fungi are attached to a surface, a multistep process starts, leading to the formation of a complex, adhering, microbial community named "biofilm". The latter involves an initial attachment step for bacteria, followed by the formation of microcolonies, and eventually differentiation of microcolonies into exopolysaccharide-encased, mature biofilms.[2,3] Biofilms cause damages and considerable costs in different fields such as medicine,[4] food and marine industries.[5] In addition, by protecting microorganisms from antimicrobial treatments, biofilms constitute a source of pathogenic infection. The development of this biofilm can be directly associated to the development of nosocomial diseases, food intoxication or biodegrations of materials. Biofilms are also responsible for a loss of hydrodynamic properties of ships, of transport properties of heat exchangers as well as of possible biocorrosion of immersed structures.

These few examples show the urgent need for undwelling innovative surface treatments which would prevent, or at least slow down, the development of biofilms.

A number of technologies have been developed to protect solid surfaces against biofilm formation. Some rely on the deposit of hydrophilic coatings [poly(ethylene glycol) (PEG) or PEG derivatives] or incorporate biocidal agents or polycations [quaternary ammonium, phosphonium, tertiary sulfonium] in polymers.[6] All these strategies are efficient and do prevent colonization; the counterpart being the cost and short duration of these strategies. Strategies, cost-effective and granting a long-term protection of materials, still need to be launched. The most common way is to attach a broad spectrum antimicrobial agent that will impede bacteria growth through usual bacteriostatic or bactericidal mechanisms.[7−11] Enzymes or other natural bactericidal substances have been used to form antibacterial coatings; they already proved their efficiency in permeabilizing membranes and stop microorganism (see refs 12 and 13 and references therein). Other authors proposed to covalently bind antimicrobial peptides [AMPs] on the surface of medical devices. Conversely, to conventional antibiotics that may be toxic, antimicrobial peptides, are natural products that are usually produced by microorganisms, fungi, plants, insects, or even animals.[14] In addition to their nontoxic origin, AMPs offer other advantages such as a broad spectrum antimicrobial activity, an action at very low concentration and, last but not least, they rarely promote a bacterial resistance.[14] Another way to prevent the toxicity of some antibacterial molecules is to graft a polymer layer which exhibits a bactericidal effect at room temperature and becomes cell-repellent only once introduced in the body.[13]

Received: June 7, 2012
Revised: September 13, 2012
Published: September 18, 2012

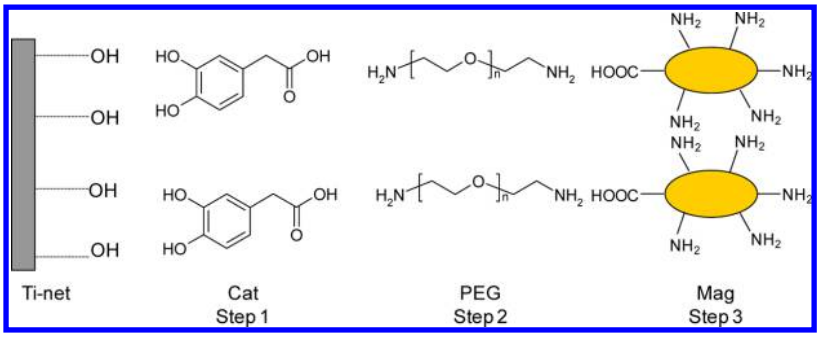

Figure 1. Scheme of the three-step functionalization process.

In several previous works, we tested the antimicrobial activity of gold surfaces functionalized by grafted Magainin I (Mag)[15] or Gramicidin A,[16] or stainless steel surfaces modified by Nisin A;[17] the two first antimicrobial peptides being produced by an amphibian, *Xenopus laevis* and a microorganism, *Lactococcus lactis*, respectively. The procedure indeed permitted 50−80% of the attachment of bacteria to be inhibited; the activity of the grafted peptide was shown to be bacteriostatic, rather than bactericidal, likely because it could not aggregate and form pores across the bacterial membrane.

In this paper, we report a multiple step functionalization strategy aiming at grafting an antimicrobial agent, the Magainin I, covalently and coupled to an antiadhesive agent, a modified poly(ethylene glycol) (PEG), on a hydroxylated titanium surface. The PEG molecule, in addition to its antiadhesive properties, acts as a cross-linker between a catechol layer, and the bioactive peptide (Magainin I). This strategy was inspired by Faure et al.'s previous work on stainless steel.[18] The use of 3,4-dihydroxyphenylalanine (DOPA) derivatives as cross-linker was shown to lead to very stable antimicrobial layers. The titanium modified surfaces were characterized step by step by means of reflection absorption infrared spectroscopy (RAIRS) and X-ray photoelectron spectroscopy (XPS). Moreover, to evaluate the antimicrobial activity of the grafted Magainin I, and/or the expected antiadhesive properties of the PEG cross-linking layers, four different tests were set up, dedicated to explore each step of the biofilm formation.

EXPERIMENTAL METHODS

Materials. 3,4-Dihydroxyphenylacetic acid (Cat-a catechol derivative, sodium chloride (NaCl), sodium citrate dihydrate (HOC-(COONa)-$(CH_2COONa)_2{\cdot}2H_2O$), *N*-hydroxysuccinimide (NHS, 1-(3-dimethylaminopropyl)-*N*-ethylcarbodiimide hydrochloride (EDC), *O*,*O*′-bis(2-aminoethyl)poly(ethylene glycol), M_w 3000 (H_2N-PEG-NH_2), and Magainin I (Mag) [Gly-Ile-Gly-Lys-Phe-Leu-His-Ser-Ala-Gly-Lys-Phe-Gly-Lys-Ala-Phe-Val-Gly-Glu-Ile-Met-Lys-Ser] were obtained from Sigma-Aldrich. Antibacterial tests were carried out with the Gram-positive bacteria *Listeria ivanovii* (Li4pVS2), which is known to form biofilms easily on several surfaces.[19] Titanium (Ti 99.6%) coupons (10 mm × 10 mm × 1 mm) were purchased from Goodfellow. All solvents were reagent-grade and were used without any further purification. *L. ivanovii* adhesion was tested at room temperature.

Preparation of Sample Surfaces. Titanium coupons were polished with an abrasive disk [abrasive grain 1200 nm] for 2 min and rinsed 1 min in milli-Q water. Then they were polished down to 1 μm (polishing disk and diamond suspension) for 2 min and ultrasonically washed 5 min in milli-Q water. Eventually, they were polished down to 0.25 μm for 15 min and successively sonicated 15 min + 10 min in milli-Q water, 10 min in acetone, 10 min in *n*-dodecane, and 10 min in 2-propanol.[20] This preparation is expected to increase the amount of hydroxyl groups on the surface.

Purification of PEG. The prepared H_2N-PEG-NH_2 polymer showed the presence of some undesired residues, evidenced on the NMR spectra (spectra not shown). Before any experiment, H_2N-PEG-NH_2 was purified. The polymer was diluted in milli-Q water. The solution was acidified with HCl to pH ∼1−2 and extracted with CH_2Cl_2 three times. Finally, the organic phase was acidified with HCl, dried over $MgSO_4$ and concentrated.[21]

Surface Functionalization. A three-step functionalization strategy was used for the elaboration of antibiofilm surfaces: first the binding of Cat, expected from the interaction of its hydroxyl groups with the surface,[21,22] followed by the deposition of H_2N-PEG-NH_2, and finally, grafting the antibacterial peptide onto the terminal groups of the functionalized PEG (Figure 1).

Cat solutions, at a concentration of 1 mg/mL, were prepared in a buffer at pH = 6 (2.61 g of NaCl and 1.32 g of sodium citrate diluted in 15 mL of milli-Q water and pH adjusted with HCl). EDC and NHS were diluted to 3.5×10^{-2} and 5.5×10^{-2} M in milli-Q water, H_2N-PEG-NH_2 solutions were prepared in milli-Q water at 2 mg/mL, and Mag was diluted in milli-Q water at 1 mg/L. These experiments were carried out at 50 °C.

For each step of surface functionalization, two series of identical samples were prepared and characterized by reflection absorption infrared spectroscopy (RAIRS) and X-ray photoelectron spectroscopy (XPS).

To graft the catechol derivative, titanium samples were immersed in a Cat solution overnight, washed for 5 min in a buffer solution and 5 min in milli-Q water, and then dried under a flow of dried air.[21] These coupons are named Ti-Cat.

Before grafting the polymer, Ti-Cat substrates were immersed in 10 mL of an EDC/NHS solution for 90 min under smooth agitation to transform the catechol carboxylic groups into reactive ester functions. They were then rinsed in milli-Q water for 5 min under agitation, leading to coupons named Ti-Cat-act.

The H_2N-PEG-NH_2 molecule was then grafted onto these Ti-Cat-act surfaces. Cat-modified titanium surfaces were immersed in the polymer solution overnight, rinsed 5 min with milli-Q water and then dried under a flow of dried air. Resulting coupons are named Ti-Cat-PEG.

Grafting of Magainin I. First, 20 μL of the Mag solution was diluted in 980 μL of EDC/NHS solution to obtain, after 90

dx.doi.org/10.1021/jp305597y | J. Phys. Chem. B 2012, 116, 13839−13847

min, 1 mL of activated Mag at 20 mg/mL. Grafting of activated Mag was then realized by depositing 100 μL of solution on Ti-Cat-PEG surfaces. After 3 h, the coupons were rinsed in milli-Q water for 10 min and dried under a flow of dried air. These coupons are named Ti-Cat-PEG-Mag.

Characterization Techniques. *Reflection–Absorption Infrared Spectroscopy (RAIRS).* RAIR spectra were recorded using a Nicolet Magna 550 FT-IR spectrometer equipped with a liquid nitrogen-cooled MCT wide-band detector (spectral range 4000–650 cm^{-1}). The sample support enabled the incidence angle to be changed. After several tests, an optimal reflection angle of 73° was chosen. All infrared spectra were recorded at 8 cm^{-1} resolution, by coaddition of 256 scans, with a background on clean titanium.[23]

X-ray Photoelectron Spectroscopy (XPS). XPS analyses were performed using a PHOIBOS 100 X-ray photoelectron spectrometer from SPECS GmbH (Berlin, Germany) with a monochromated Al Kα X-ray source ($h\nu$ = 1486.6 eV) operating at $P = 1 \times 10^{-10}$ Torr or less. Spectra were carried out with a 50 eV pass energy for the survey scan and 10 eV pass energy for the C1s, O1s, N1s, and Ti2p regions. High-resolution XPS conditions have been fixed: "fixed analyzer transmission" analyses mode, a 7 × 20 mm entrance slit, leading to a resolution of 0.1 eV for the spectrometer, and an electron beam power of 150 W (15 kV and 10 mA). A takeoff angle of 90° from the surface was employed for each sample. Element peak intensities were corrected by Scofield factors.[24] The spectra were fitted using Casa XPS v.2.3.15 Software (Casa Software Ltd.) and applying a Gaussian/Lorentzian ratio G/L equal to 70/30.

Atomic Force Microscopy Imaging (AFM). AFM images of dried surfaces were recorded using a di Caliber AFM microscope from Bruker Instruments Inc. To avoid tip and sample damages, topographic images were taken in the noncontact dynamic mode also known as tapping. Silicon nitride tips (resonance frequency 280–400 kHz, force constant 40–80 N/m) have been used. Images were obtained at a constant speed of 2 Hz with a resolution of 512 lines and 512 pixels each. The raw data were processed using the imaging processing software di SpmLabAnalysis v.7.0 from Veeco Instruments Inc., mainly to correct the background slope between the tip and the titanium surface.[15]

Tests of Surface Antibiofilm Activity. The formation of a biofilm is known to occur following several steps (Figure 2).[1] It starts with the adsorption of proteins present in the environment of the metallic surface. Microorganisms then easily adhere on this layer and grow, forming colonies by using these proteins as nutrient. Adhesion and growth of bacterial cells thus constitute two steps to be interrogated. Once the biofilm is formed, microorganisms are often protected by the matrix from antibiotic or any other sources of aggression, resulting in a "stable" biofilm, and this has to be tested as well.[25] To evaluate the antibiofilm effect of the new elaborated surface coating, and to better identify the step that is most inhibited, if it is, a set of specific tests was designed and conducted as described here below.

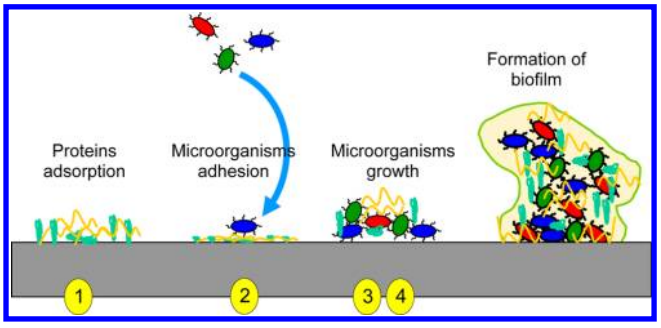

Figure 2. Consecutive steps of the formation of a biofilm on surface.

1. Adsorption of Proteins (Test 1). The first test aimed at measuring the effect of H_2N-PEG-NH_2 in preventing protein adsorption. A bovine serum albumin (BSA) solution in milli-Q water was prepared at 0.1 mg/mL. Ti, Ti-Cat, and Ti-Cat-PEG samples were immersed in this solution for 1 h at room temperature and under agitation. The samples were then rinsed for 5 min in milli-Q water and dried under a flow of dried air. The surfaces were then analyzed by RAIRS, and the amounts of BSA, adsorbed on clean Ti, Ti-Cat, Ti-Cat-PEG, or Ti-Cat-PEG-Mag surfaces were compared by considering the intensities of amide bands, the proteins IR fingerprints.

2. Adhesion of Bacteria (Test 2). Following protein adsorption, the process of biofilm formation implies adhesion of microorganisms. If the latter is inhibited, biofilms will not grow. Test 2 was thus elaborated to assess the antiadhesive properties of H_2N-PEG-NH_2 and Mag against microorganisms in solution.

Nonpathogenic bacteria, *L. ivanovii* Li4pVS2, were first grown at 37 °C in brain heart infusion (BHI) broth overnight. The activity of functionalized surfaces against bacteria was tested following a methodology described in a previous work.[26] A 100 μL drop, containing 10^8 bacteria, was deposited on Ti, Ti-Cat-PEG and Ti-Cat-PEG-Mag samples and left for 3 h at 25 °C under a wet atmosphere to avoid evaporation. Importantly, under these conditions, bacteria cannot grow; thus only the effect of bacteria adhesion on the surfaces is tested. Samples were then washed with 6 × 100 μL of milli-Q water and dried under a flow of dried air. The amount of bacteria adhered on the surface was then controlled by RAIRS.

3. Viability of Bacteria (Test 3). In the process of biofilm formation, after microorganism adhesion, the latter start excreting exopolymers, and this is only possible when bacteria remain alive after adhesion. Test 3 thus consists in analyzing and comparing the viability of bacteria after having been in contact with either a clean or a Mag-functionalized surface. We used the same conditions as for Test 2 (3 h at 25 °C) to test the viability of bacteria once adhered. Bacteria were then observed by atomic force microscopy, which enables us to detect possible shape changes or cell wall damages. Note that AFM images were recorded in the air, after surface drying, and not in the cell solution; this is compatible with our objective, sometimes even preferable, when willing to characterize a bacteria film and observe topographic features on cells, avoiding capillary effects.[27,28]

4. Growth of Bacteria (Test 4). The final step in the biofilm formation is reached if bacteria grow and form aggregates. With the last test (Test 4), the inhibitor activity of H_2N-PEG-NH_2 and Mag on bacteria growth was measured doing a CFU (colony-forming unit) counting after detachment of the bacterial layers from surfaces.[15] 100 μL of culture solution, containing 10^8 bacteria, were deposited on Ti, Ti-Cat, Ti-Cat-PEG, and Ti-Cat-PEG-Mag samples for 3 h at 37 °C under wet atmosphere. Contrary to test 2 and 3 conditions, these permit the growth of bacteria; test 4 thus reveals the inhibition, or the delay, of bacteria growth induced by the presence of organic layers. Samples were washed three times with physiological

dx.doi.org/10.1021/jp305597y | J. Phys. Chem. B 2012, 116, 13839–13847

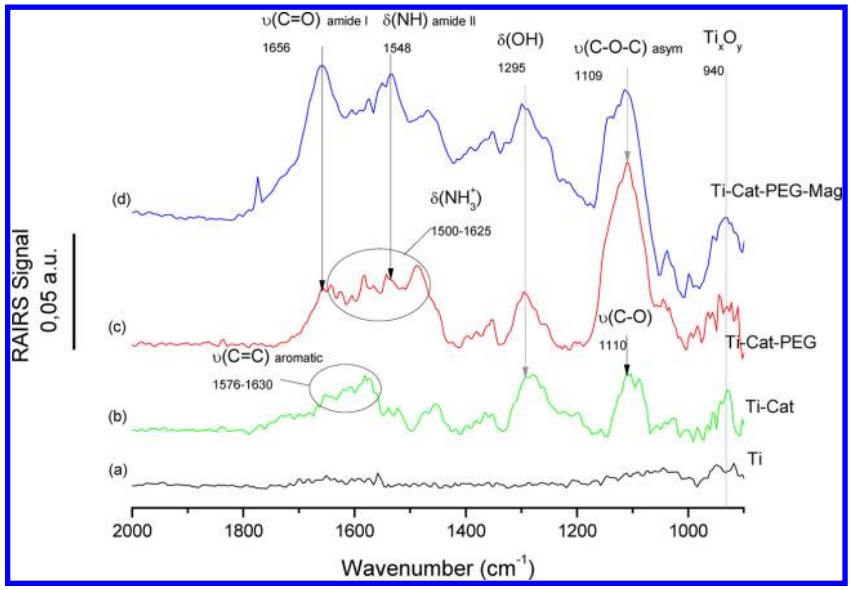

Figure 3. FT-RAIRS spectra after successive steps of functionalization: (a) Ti, (b) Ti-Cat, (c) Ti-Cat-PEG, and (d) Ti-Cat-PEG-Mag.

sterile solution (0.9% NaCl) to remove nonadhered bacteria. Then, they were sonicated in 2 mL of physiological sterile solution for 3 min at 60 W to retrieve nothing but bacteria which have adhered to the surfaces. After sonication, the bacteria were pelleted by centrifugation at 10000 *g* for 5 min. Then 1.8 mL of supernatant was removed cautiously and the bacteria were resuspended by vortexing. The suspension was then diluted 100 times; 50 μL of each dilution were deposited on BHI agar plates (15 g/L), in duplicate for each dilution, using a spiral plater WASP [AES, France]. Before counting colonies, the plates were incubated at 37 °C for 24 h. After incubation, we counted the colonies on each plates and calculated a percentage of inhibition of bacteria growth regarding the reference on Ti with the following formula:

$$\%\ \text{Inhibition}_{\text{sample}} = \left(1 - \frac{\text{CFU}_{\text{sample}}}{\text{CFU}_{\text{Ti}}}\right) \times 100$$

RESULTS

Step 0: Characterization of Clean Titanium. Before any functionalization, clean titanium surfaces were characterized by RAIRS and XPS. Figure 3a shows a typical RAIRS spectrum collected after polishing and washing Ti samples. Only weak bands related to titanium oxides at 940 cm^{-1} were observed.[29] As for XPS, the Ti 2p$_{3/2}$ peak (see Supporting Information) could be decomposed into two components: a major one at 459.0 ± 0.1 eV attributed to titanium in TiO_2, and a weak one at 454.0 ± 0.1 eV attributed to metallic titanium.[30] The O 1s peak (Figure 4) confirmed the presence of titanium dioxide; the intense O 1s peak at 530.6 ± 0.1 eV is attributed to the TiO_2 oxide film;[30] some traces of organic contamination are evidenced by a weak peak at 532.0 ± 0.1 eV attributed to oxygen in C═**O** bonds.[31]

Step 1: Grafting of Catechol. Figure 3b presents typical RAIRS spectra recorded after treatment in a Cat solution. In comparison with Figure 3a, Figure 3b shows several characteristic bands: a medium ν_{C-O} band at 1110 cm^{-1} and a broad δ_{OH} band at 1295 cm^{-1} related to carboxylic acid groups; in addition, a broad massif at 1575−1630 cm^{-1} could be attributed to the C═C stretching band of the catechol aromatic rings.[32] The Ti$_x$O$_y$ band, at 940 cm^{-1}, was still detectable.

Ti-Cat samples were also analyzed by XPS and the resulting spectra are presented in Figure 4. The O 1s peak was decomposed into three main components, at 530.6 ± 0.1, 532.0 ± 0.1, and 533.5 ± 0.1 eV, easily attributed to oxygen in titanium oxide, in (C═**O**)—OH, and in (C═O)—**O**H bonds, respectively; a very weak contribution was observed at 536.5 ± 0.1 eV, which we already saw on other titanium oxide samples, without explaining it unambiguously; it might also be due to the oxygen atoms in α position of the phenyl.[33] The TiO_2 oxygen peak decreased, compared to that observed on clean samples, whereas the other components evidence the presence of organic molecules on the surface. The carbon C 1s peak was best fitted with four components, a dominant one at 285.3 ± 0.1 eV corresponding to carbon in **C**—(C,H)bonds and three smaller ones; one, centered at 286.7 ± 0.1 eV is attributed to carbon bound to nitrogen or oxygen (**C**—N and **C**—O), the second at 288.6 ± 0.1 eV to carbon in (**C**═O)—(O,N) groups and the latter at 290.2 ± 0.1 eV is the satellite peak characteristic of the benzyl $\pi \rightarrow \pi^*$ transition.[34,35]

Step 2: Grafting of Diamine Poly(ethylene glycol). The grafting of H_2N-PEG-NH_2 relies on the formation of peptidic bonds between the amine group of the polymer and the activated carboxylic acid of Cat.

Figure 3c shows RAIRS spectra recorded after reaction of H_2N-PEG-NH_2 with the surface. The growth of an intense massif centered at 1109 cm^{-1}, easily attributed to the ν_{C-O-C} asymmetric band at, and of $\delta_{NH_3^+}$ bands detected at 1500 and 1625 cm^{-1}, are strong indications of the fixation of H_2N-PEG-NH_2. Additional features, at 1548 and 1656 cm^{-1}, which can be associated respectively to $\nu_{C=O}$ (amide I) and a combination of δ_{NH} and $\nu_{C=N}$ (amide II), confirm the covalent grafting of the second PEG layer.[36]

XPS analysis of Ti-Cat-PEG samples (Figure 4) confirms RAIRS results, with O1s and C 1s peaks characteristic of the organic layer and an intense N 1s signal. When comparing results to the XPS spectra after catechol adsorption, one notes the decrease of the two lower O1s BE contributions, related to the oxide, and to (C═O)—**O**H groups; at the same time, two

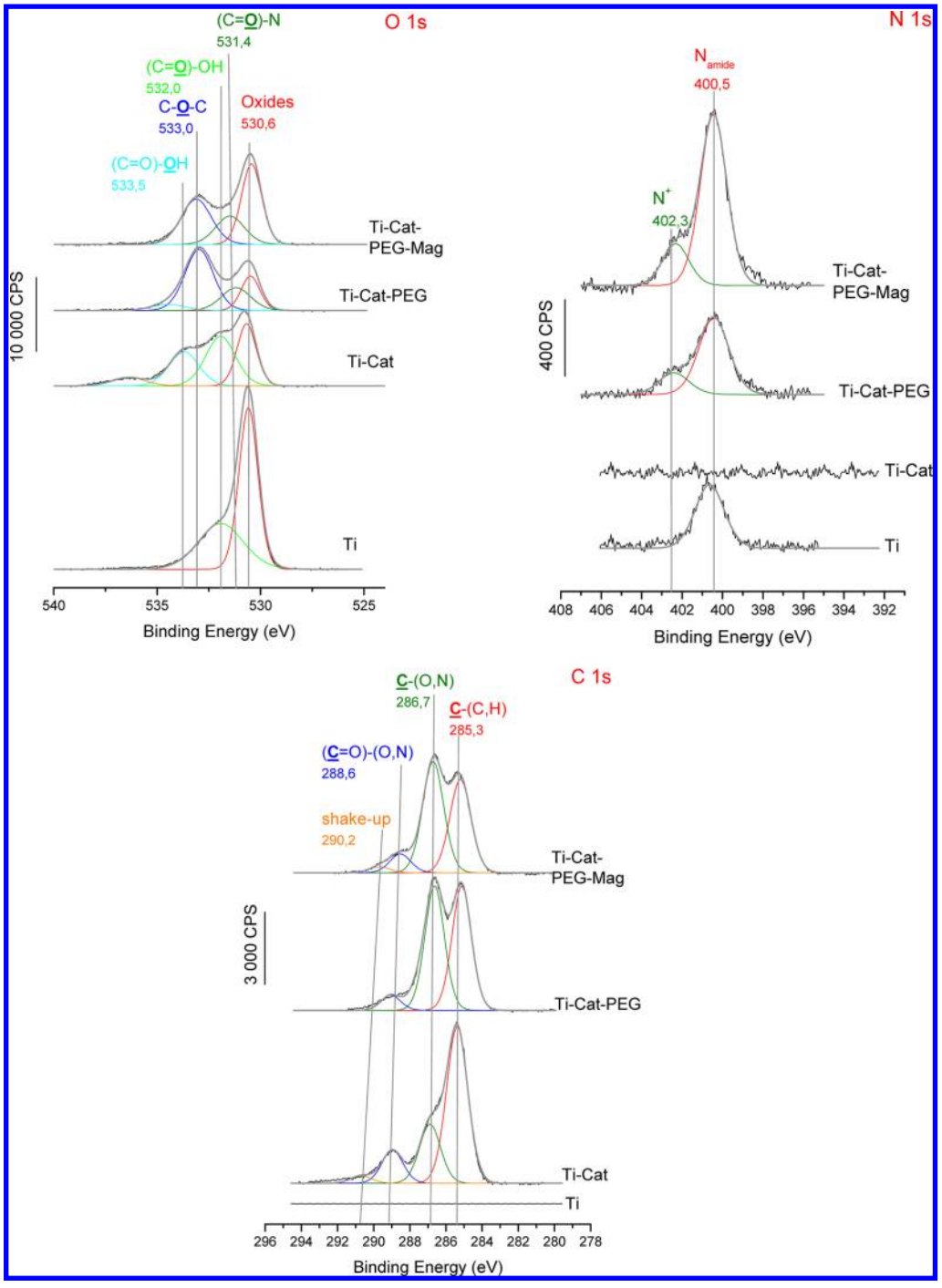

Figure 4. XPS spectra of the O 1s, N 1s, and C 1s regions for (from bottom to top) Ti, Ti-Cat, Ti-Cat-PEG, and Ti-Cat-PEG-Mag.

new peaks show up, at 531.4 ± 0.1 and 533.0 ± 0.1 eV corresponding to oxygen in amide bands (C═**O**)—N and C—**O**—C groups, respectively.

A new N 1s signal is detected that could be decomposed in two components: an intense peak at 400.3 ± 0.1 eV attributed to the nitrogen in amide bonds or possibly to NH_2 and a smaller one at 402.3 ± 0.1 eV corresponding to NH_3^+ groups. Eventually, a net increase of the carbon contribution at 286.7 ± 0.1 eV is obviously due to the presence of C−O−C bonds on the surface. All these data are strong indications of the formation of a H_2N-PEG-NH_2 adlayer.[36]

Step 3: Grafting of Magainin I. The grafting of Mag is expected by reaction of an activated Glutamic acid moiety of Mag with adsorbed H_2N-PEG-NH_2 .

Figure 3d displays RAIRS spectra recorded after that step. The ν_{C-O-C} stretching band at 1109 cm^{-1} is still detected but new bands appear at 1656 and 1548 cm^{-1}, which can be attributed to the amide I ($\nu_{C=O}$) and amide II ($\delta_{NH} + \nu_{C-N}$) signals, respectively. Magainin I is a peptide, constituted of amino acids linked one to the other via peptidic bonds, likely at the origin of these new signals.[15] Absorption signals at ca. 1400, 1600, and maybe 1700 cm^{-1}, easily attributed to the symmetric and asymmetric COO^- stretching bands, and to the C═O

dx.doi.org/10.1021/jp305597y | J. Phys. Chem. B 2012, 116, 13839−13847

stretch, are also present on the spectrum, thus confirming the presence of Mag on top of the PEG layer.

The XPS analysis (Figure 4), shows an increase of peaks that can be related to the presence of Mag: the O 1s peak attributed to oxygen in C═**O** bonds at 531.4 ± 0.1 eV, the N 1s peak related to nitrogen in amide bonds at 400.5 ± 0.1 eV, and the C 1s peak due to carbon in (**C**═O)—N groups at 288.6 ± 0.1 eV.[15] We also noticed a slight decrease of the C—**O**—C peak at 533.0 ± 0.1 eV, explained by an attenuation of the PEG layer by Mag. The average thickness of each layer, d, was calculated from the successive attenuations of the titanium signal, using the following equation:

$$\frac{I}{I_0} = \exp\left(-\frac{d}{\lambda}\sin\varphi\right)$$

where I and I_0 are the Ti 4f peak intensity before and after adsorption of a given layer respectively, λ is the mean free path of the Ti 4f electron through an organic layer. The obtained value for the final Mag layer was close to 20 Å thick, whereas the Magainin I medium radius lies between 25 and 30 Å depending on the solvation sphere.[37]

Both RAIRS and XPS analyses confirm the binding of Mag, and also show that the amount of anchored peptides is rather weak, below a complete layer from which much more intense signals, and stronger substrate attenuation would be expected.

Antifouling and Antimicrobial Activities. Four tests, described in the Experimental Methods, were successively conducted to evaluate the antifouling and antimicrobial activities of the successively grafted layers.

1. Test 1: Antiadhesive Effect of H_2N-PEG-NH_2 Layer toward Protein Adsorption. First, adsorption of proteins was tested using BSA, a protein known to easily adsorb on many types of surfaces.[38,39] Figure 5 shows the RAIRS spectra, in the region of the protein characteristic amide bands, recorded after deposition of BSA solution and rinsing, on Ti, Ti-Cat, and Ti-Cat-PEG surfaces. Each shown spectrum is the result of a subtraction of the spectra after and before BSA interaction on a given type of surface; thus only changes due to BSA interaction are expected to be present. Indeed, on all spectra, bands at ca. 1550 and 1650 cm^{-1}, ascribed to adsorbed BSA, are present.

Their intensity, directly related to the amount of adsorbed BSA, is roughly the same on clean titanium and Cat-modified surfaces, whereas it is reduced, by a factor of 4, on the PEG functionalized surface.

2. Test 2: Antiadhesive Effect of H_2N-PEG-NH_2 and Mag toward Bacteria Adhesion. Having shown the antiprotein adsorption activity of H_2N-PEG-NH_2 surfaces, this second test is expected to probe adhesion of bacteria on all functionalized surfaces. To do so, a solution of *L. ivanovii* was deposited on Ti, Ti-Cat-PEG, and Ti-Cat-PEG-Mag samples, as described in the Experimental Methods. After being rinsed and dried, the samples were analyzed with RAIRS; antiadhesive properties of functionalized samples were then compared to those of clean titanium samples.

Figure 6a shows the RAIRS spectra of the three types of surfaces, Ti, Ti-Cat-PEG, and Ti-cat-PEG-Mag, after contact with a solution of bacteria. On the clean titanium surface, one sees intense bands which are indeed bacterial markers, the C—O—C stretching of membrane carbohydrates at 1085 cm^{-1}, the C—O—P stretching of polysaccharides also contained in the membrane, at 1242 cm^{-1};[40] bands at 1403, 1556, and at 1662 cm^{-1} can be respectively attributed to the symmetric COO^-

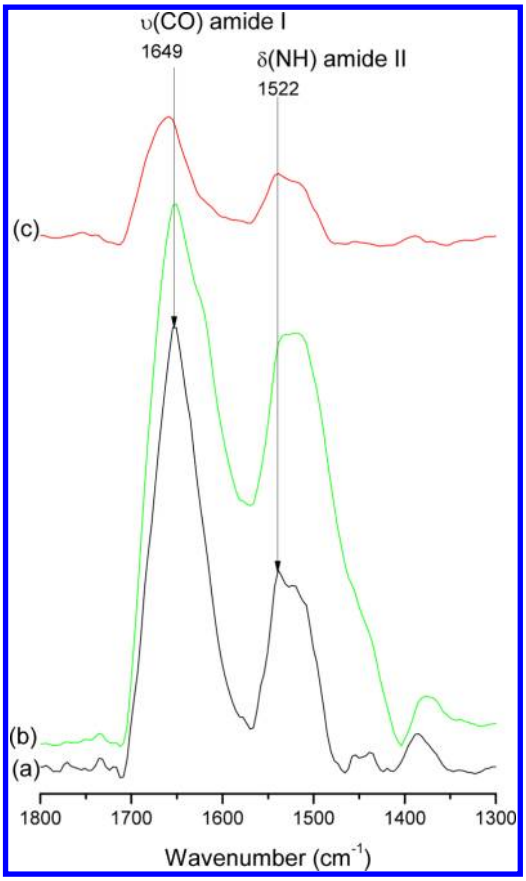

Figure 5. FT-RAIRS spectra of (a) Ti, (b) Ti-Cat, and (c) Ti-Cat-PEG after deposition of BSA.

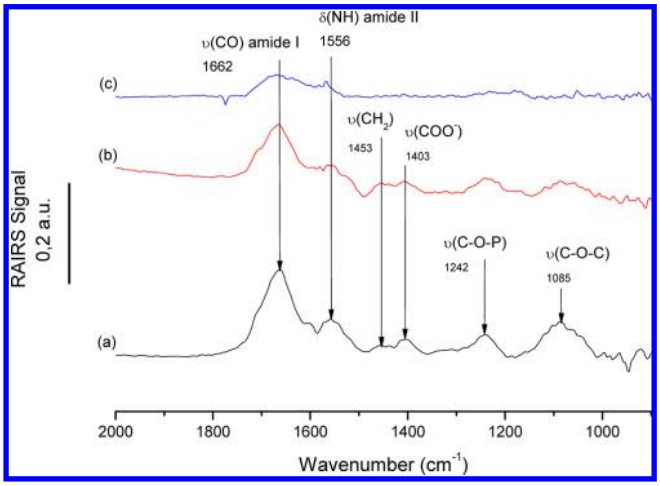

Figure 6. FT-RAIRS spectra of (a) Ti, (b) Ti-Cat-PEG and (c) Ti-Cat-PEG-Mag after bacteria deposition.

stretching, ν_{COO-}, of fatty acids,[41] and to the two amide bands, $\delta_{NH} + \nu_{C-N}$, (amide II) and $\nu_{C=O,}$ (amide I).[42] Figure 6b shows a net decrease of these intensity bands, by a factor close to two. On the Ti-Cat-PEG-Mag surface (Figure 6c), only very weak amide bands at 1662 and 1556 cm^{-1} are still detected. The H_2N-PEG-NH_2 and the Mag modified surfaces do have an antiadhesive effect toward bacteria.

3. Test 3: Viability of Bacteria Adhered on the Surfaces. As deduced from Test 2, Ti-Cat-PEG-Mag surfaces have a significant, but not total, inhibiting effect on bacteria adhesion.

dx.doi.org/10.1021/jp305597y | J. Phys. Chem. B 2012, 116, 13839−13847

The question is thus whether these adhered bacteria are still alive and prone to develop on the surface, or significantly damaged. The followed test thus aims at the observation of adhered bacteria. After deposition of *L. ivanovii* on Ti, Ti-Cat-PEG, and Ti-Cat-PEG-Mag surfaces, the latter have been imaged by AFM. The highest images of Figure 7 show first the

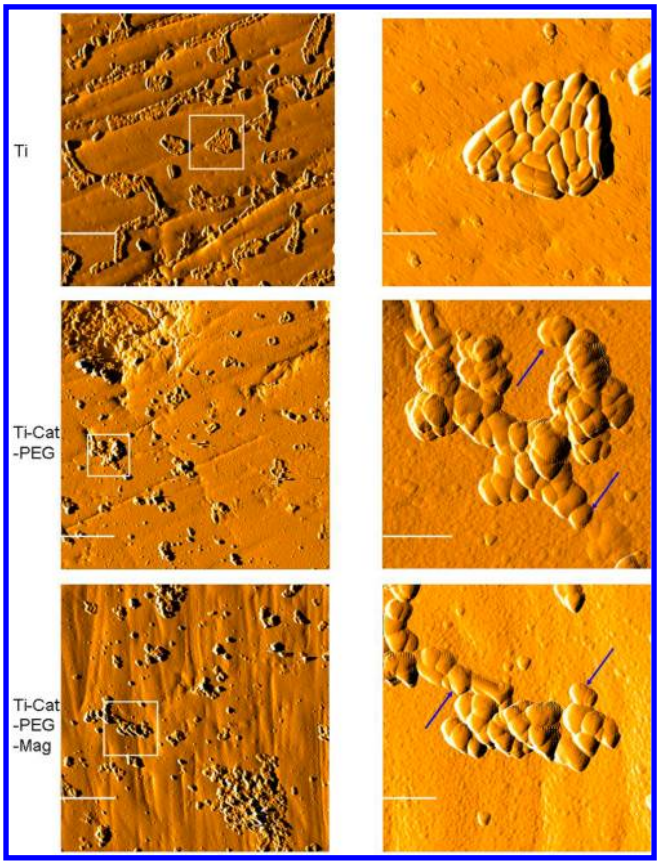

Figure 7. AFM images of Ti, Ti-Cat-PEG, and Ti-Cat-PEG-Mag after bacteria deposition. Left images: scale bar = 10 μm and right images: scale bar = 2 μm.

topography of clean Ti surfaces after deposition of bacteria, at two different scales. One observes that bacteria, adhered to the surface, form aggregates keeping their elongated and rather thick native shape.[43] Intermediate images of Figure 7, obtained on Ti-Cat-PEG surfaces after bacteria deposition, again show aggregation of bacteria; noticeable is their less well-defined shape as if some bacteria were partially crashed, or preferentially deposited on top of an already adhered one. Eventually, in the lowest images of Figure 7, recorded on Ti-Cat-PEG-Mag surfaces, bacteria have lost their native shapes; they appear to be crashed and, for some of them (see arrows on Figure 7), depleted of their contents. These images suggest that Mag and H_2N-PEG-NH_2 have a detrimental effect on bacteria, by damaging their membranes.

4. Test 4: Inhibition of Bacteria Growth. Damaging bacteria membranes does not imply a death of cells; the latter may recover and develop again when the surrounding conditions change.[44] The last test, consisting in counting bacteria after contact with modified surfaces and treatment in a growth solution, was thus essential.

To do so, about 10^8 bacteria were deposited on clean Ti, Ti-Cat, Ti-Cat-PEG, and Ti-Cat-PEG-Mag samples; after 3 h at 37 °C, adhered cells were detached from the surfaces by sonication and the number of CFU per mL counted. We thus measured and compared the numbers of alive bacteria, after contact with the variously functionalized surfaces. As shown in Figure 8a, the number of CFU, after adhesion onto clean Ti, is higher than on any of the modified surfaces. A slight decrease was observed on Ti-Cat whereas, on Ti-Cat-PEG, the number of alive bacteria cells was decreased by a factor of 2. The most severe reduction has been observed on Ti-Cat-PEG-Mag with ca. 1 order of magnitude difference compared to the result on Ti. The comparison is easier by considering the percentages of inhibition of bacteria growth on the so-elaborated surfaces (Figure 8b) as compared growth on Ti substrates. We noticed a decrease of bacteria growth by ca. 70% on Ti-Cat-PEG and 90% on Ti-Cat-PEG-Mag. We also observed that the Cat moiety seems to have an effect with a percentage of inhibition around 55%. The results were reproduced by using two different sets of functionalized samples and culture batches of each strain. These results demonstrate that, though a possible variability on the results on Ti-Cat and Ti-Cat-PEG surfaces, there is a clear inhibition of cell development due to the PEG polymer, and an even more severe one in the presence of Magainin I.

DISCUSSION

First, PEG and Magainin I were successfully grafted on titanium surfaces in a 3-step functionalization process. Step 1 consisted in the pseudocovalent grafting of a Cat derivative onto titanium surfaces. This grafting results from the formation of a charge transfer complex between the two hydroxyl groups of the Cat molecule and the hydroxyl groups present on the clean titanium surface.[21,22] Thanks to the rather rigid aromatic cycle and associated good arrangement of the organic layer, we expect a good accessibility of the carboxylic acid groups. Grafting of NH_2−PEG-NH_2 on Ti-Cat surfaces was clearly demonstrated by RAIRS and XPS results. The detection of a C−O−C band at 1109 cm^{-1}, and of NH_3^+ around 1600 cm^{-1}, confirms the grafting of the polymer and the accessibility of the amine group for the next step. The increase of the nitrogen N1s peak at 400.4 ± 0.1 eV, together with the decrease of the titanium Ti $2p_{3/2}$ peak, after deposition of NH_2−PEG-NH_2 are another proof of the PEG grafting. Note that in a previous work, Yuan et al.[45] have modified stainless steel surfaces with dopamine, and they had to modify the latter with an alkyl bromide ATRP initiator before grafting a PEGMA (poly(ethylene glycol) methacrylate) macromonomer. Fan et al.[20] also used a bromide modified initiator to achieve a polymerization directly onto titanium surfaces. Using the direct polymerization permits us to vary the length of the polymer and to control the grafting of this molecule on the Cat precursor. Other research groups[21,46] synthesized the DOPA initiator together with the polymer before grafting the whole molecule. This is also a good way to control the reaction between the two components, but it might make the anchoring to the surface more difficult. The advantage of our two-step process is 2-fold: first, an homogeneous, though likely multilayered, Cat film could be obtained with a single molecule; second, soft and easy to handle conditions were sufficient to graft the NH_2−PEG-NH_2 molecule. It is, however, true that we could not influence the length of the polymer.

Eventually, the grafting of Magainin I on Ti-Cat-PEG surfaces is confirmed by RAIRS with the increase of amide I band at 1656 cm^{-1} and the increase of N1s peak at 400.4 ± 0.1 eV in the XPS analysis. We, however, observed a small increase of C 1s peak related to carbon in amide groups, at 288.6 ± 0.1

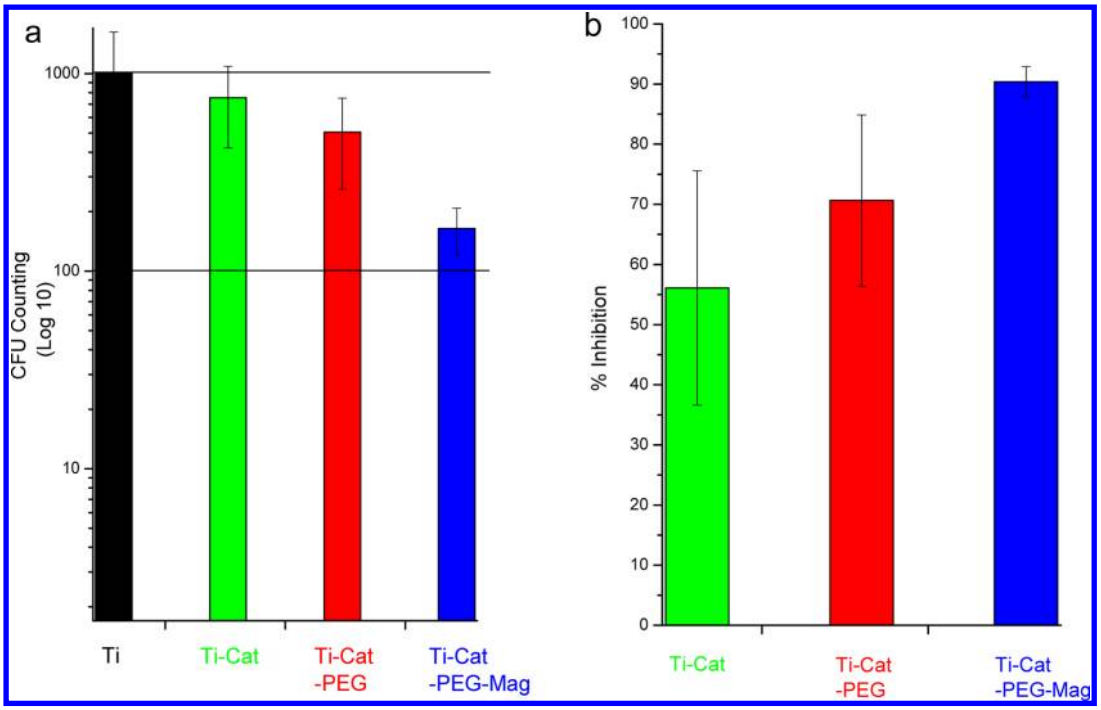

Figure 8. (a) CFU counting of *L. ivanovii* on Ti-Cat, Ti-Cat-PEG, and Ti-Cat-PEG-Mag. Error bars indicate standard deviation from two independent CFU counting. (b) Inhibition of the growth of *L. ivanovii* on Ti-Cat-PEG and Ti-Cat-PEG-Mag surfaces as compared to growth on Ti-Cat substrates. Percentages correspond to % = $(1- (CFU_{sample}/CFU_{Ti})) \times 100$.

eV, and a very slight decrease in Ti $2p_{3/2}$ XPS peak, after grafting the Magainin I. These small modifications suggests that a very small amount of Magainin I has been grafted, far from covering the whole surface. This could be explained by the formation of a PEG loop between two Cat moieties due to the bifunctionality of the polymer. We may also have Magainin I aggregates that would explain the little attenuation of the titanium XPS signal. Yet, in previous work, Brooks et al. showed that the antimicrobial activity of a surface was higher when the chain flexibility is limited, the polymer layer is thick and most important the peptide density on the surface is high.[47] There might be a need to improve the amount of immobilized Magainin molecules. One may think of a four-step process as reported by Héquet et al.[17] using a dialdehyde cross-linker between the polymer layer and the Magainin I[17] or try to functionalize the Magainin I with a more reactive molecule as Glinel et al. did.[48] Before trying other protocols, important was to assess the antibiofilm activity of the successively functionalized surfaces. This constitutes an innovative part of this work, setting up various tests to measure the inhibiting effect of the functionalized surfaces toward one or several steps of the formation of a biofilm.

First, we tested the effect of grafting the PEG toward protein adsorption. By comparing the intensity of amide bands, we observed a net decrease of BSA adsorption on PEG-modified samples. This confirms the antiadhesive effect of a PEG-containing layer. This well-known property might be due to the chain mobility of H_2N-PEG-NH_2, a large excluded volume and high hydrophilicity.[49] Note, however, that the observed decrease is smaller than reported in previous studies, likely due to the smaller chain of the utilized H_2N-PEG-NH_2[2,45] or to the structure of the modified polymer.[36] This result could be improved by modifying the length and/or the synthesis of the H_2N-PEG-NH_2 molecule.

We then tested the influence of PEG and Magainin I on bacteria adhesion. A significant decrease of bacteria adhesion was observed on Ti-Cat-PEG, and even more on Ti-Cat-PEG-Mag. The antiadhesive effect of the Magainin may be due to the presence of a protonated amine group at the end of the peptide, positive charges being known to have repellent properties against bacteria.[50] Despite the significant antiadhesive properties of combined adsorbed PEG and Magainin, the RAIR spectrum makes clear the presence of some bacteria still adhering to the surface. AFM images recorded on clean titanium, and on PEG + Mag-functionalized surfaces, after bacteria deposition, confirmed that, on clean surface bacteria keep their native shape whereas on Ti-Cat-PEG-Mag they look damaged. The final test, consisting in assaying the viability of adhered bacteria, by CFU counting, is indeed informative ... and impressive: only 10−30% of the adhered bacteria on functionalized surfaces can be revivified; note that this may be sufficient to create in fine a biofilm, but probably on a long time frame.

■ CONCLUSIONS

This paper reports an innovative route to immobilize antiadhesive and bactericidal molecules on an oxide surface. RAIRS and XPS analyses were applied at each step of surface modification leading to the following conclusion: PEG and Magainin I can be covalently bound to an oxidized titanium surface via a catechol derivative layer, making the surface both protein-repellent and bactericidal. Although the coverage of Magainin I was low, one observed a significant decrease of bacteria adhesion, and of the viability of the limited amount of adhered cells. The established strategy appears to be an interesting way for combining antiadhesive and antimicrobial properties on a oxide surface. Such results have implications for surface coating development for various applications, such as food preservation or medical instruments for example.

As a prospective, confocal microscopy could be used to confirm and quantify results about alive or dead bacteria on modified surfaces. Another strategy using enzymes, such as Hen Egg White Lysozyme, instead of antibacterial peptides is under study. Enzymes have a different action mode compared to the action of peptides, for instance, lysozymes hydrolyze the membrane of Gram-positive bacteria, thus enhancing the bactericidal property of the so-modified surface. It would be interesting to compare the antibacterial activities of peptides and enzymes and correlate the results to their mode of operation.

■ ASSOCIATED CONTENT

Supporting Information

XPS spectra of the Ti2p regions for Ti, Ti-Cat, Ti-Cat- PEG, and Ti-Cat-PEG-Mag. This material is available free of charge via the Internet at http://pubs.acs.org.

■ AUTHOR INFORMATION

Corresponding Author

*E-mail: claire-marie.pradier@upmc.fr. Tel: +33 (0)1 44 27 55 33. Fax: +33 (0)1 44 27 60 33.

Notes

The authors declare no competing financial interest.

■ ACKNOWLEDGMENTS

The Centre National de la Recherche Scientifique (CNRS) and the Délégation Générale pour l'Armement (DGA) are acknowledged for J.P. Ph.D. funding.

■ REFERENCES

(1) Sauer, K.; Camper, A. K.; Ehrlich, G. D.; William, J.; Davies, D. G.; Costerton, J. W. *J. Bacteriol.* **2002**, *184*, 1140−1154.
(2) Costerton, J. W.; Zbigniew, L. *Annu. Rev. Microbiol.* **1995**, *49*, 711−745.
(3) O'Toole, G.; Kaplan, H. B.; Kolter, R. *Annu. Rev. Microbiol.* **2000**, *54*, 49−79.
(4) Hall-Stoodley, L.; Costerton, J. W.; Stoodley, P. *Nat. Rev. Microbiol.* **2004**, *2*, 95−108.
(5) Beech, I. B. *Int. Biodeter. Biodeg.* **2004**, *53*, 177−183.
(6) Kanazawa, A.; Ikeda, T.; Endo, T. *J. Polym. Sci. A Polym. Chem.* **1993**, *31*, 335−343.
(7) Klibanov, A. M. *J. Mater. Chem.* **2007**, *17*, 2479−2482.
(8) Kohnen, W. *Biomaterials* **2003**, *24*, 4865−4869.
(9) Lee, D.; Cohen, R. E.; Rubner, M. F. *Langmuir* **2005**, *21*, 9651−9659.
(10) Lichter, J. A.; Rubner, M. F. *Langmuir* **2009**, *25*, 7686−7694.
(11) Tiller, J. C.; Liao, C. J.; Lewis, K.; Klibanov, A. M. *Proc. Natl. Acad. Sci. U. S. A.* **2001**, *98*, 5981−5985.
(12) Glinel, K.; Thebault, P.; Humblot, V.; Pradier, C. M.; Jouenne, T. *Acta Biomater.* **2012**, *8*, 1670−1684.
(13) Laloyaux, X.; Fautré, E.; Blin, T.; Purohit, V.; Leprince, J.; Jouenne, T.; Jonas, A. M.; Glinel, K. *Adv. Mater.* **2010**, *22*, 5024−5028.
(14) Hancock, R. E. W.; Sahl, H.-G. *Nat. Biotechnol.* **2006**, *24*, 1551−1557.
(15) Humblot, V.; Yala, J.-F.; Thebault, P.; Boukerma, K.; Héquet, A.; Berjeaud, J.-M.; Pradier, C.-M. *Biomaterials* **2009**, *30*, 3503−3512.
(16) Yala, J.-F.; Thebault, P.; Héquet, A.; Humblot, V.; Pradier, C.-M.; Berjeaud, J.-M. *Appl. Microbiol. Biotechnol.* **2011**, *89*, 623−634.
(17) Héquet, A.; Humblot, V.; Berjeaud, J.-M.; Pradier, C.-M. *Colloids Surf. B* **2011**, *84*, 301−309.
(18) Faure, E.; Lecomte, P.; Lenoir, S.; Vreuls, C.; Van De Weerdt, C.; Archambeau, C.; Martial, J.; Jérôme, C.; Duwez, A. S.; Detrembleur, C. *J. Mater. Chem.* **2011**, *21*, 7901−7904.
(19) Vázquez-Villanueva, J.; Orgaz, B.; Ortiz, S.; López, V.; Martínez-Suárez, J. V.; SanJose, C. *Zoonoses and Public Health* **2010**, *57*, 402−410.
(20) Fan, X.; Lin, L.; Messersmith, P. B. *Biomacromolecules* **2006**, *7*, 2443−2448.
(21) Dalsin, J. L.; Lin, L.; Tosatti, S.; Vörös, J.; Textor, M.; Messersmith, P. B. *Langmuir* **2005**, *21*, 640−646.
(22) Rodriguez, R.; Blesa, M. A.; Regazzoni, A. E. *J. Colloid Interface Sci.* **1996**, *177*, 122−131.
(23) Humblot, V.; Méthivier, C.; Pradier, C.-M. *Langmuir* **2006**, *22*, 3089−3096.
(24) Scofield, J. H. H. *J. Electron Spectrosc. Relat. Phenom.* **1976**, *8*, 129−137.
(25) Djordjevic, D.; Wiedmann, M.; McLandsborough, L. A. *Appl. Environ. Microbiol.* **2002**, *68*, 2950−2958.
(26) Caro, A.; Humblot, V.; Méthivier, C.; Minier, M.; Salmain, M.; Pradier, C.-M. *J. Phys. Chem. B* **2009**, *113*, 2101−2109.
(27) Binggeli, M.; Mate, C. M. *Appl. Phys. Lett.* **1994**, *65*, 415−417.
(28) Bolshakovaa, A. V.; Kiselyovaa, O. I.; Filonova, A. S.; Frolovab, O. Y.; Lyubchenkoc, Y. L.; Yaminsky, I. V. *Ultramicroscopy* **2001**, *86*, 121−128.
(29) Guo, Q.; Oh, W. S.; Goodman, D. W. *Surf. Sci.* **1999**, *437*, 49−60.
(30) Kumar, P. M.; Badrinarayanan, S.; Sastry, M. *Thin Solid Films* **2000**, *358*, 122−130.
(31) Li, S.-C.; Losovyj, Y.; Diebold, U. *Langmuir* **2011**, *27*, 8600−8604.
(32) Gulley-Stahl, H.; Hogan, I. P. A.; Schmidt, W. L.; Wall, S. J.; Buhrlage, A.; Bullen, H. A. *Environ. Sci. Technol.* **2010**, *44*, 4116−4121.
(33) Clark, D. T.; Thomas, H. R. *J. Polym. Sci., Part A: Polym. Chem.* **1978**, *16*, 791−820.
(34) Fleutot, S.; Dupin, J.-C.; Renaudin, G.; Martinez, H. *Phys. Chem. Chem. Phys.* **2011**, *13*, 17564−16578.
(35) Rodenstein, M.; Zürcher, S.; Tosatti, S. G. P.; Spencer, N. D. *Langmuir* **2010**, *26*, 16211−16220.
(36) Huang, N.-P.; Michel, R.; Voros, J.; Textor, M.; Hofer, R.; Rossi, A.; Elbert, D. L.; Hubbell, J. A.; Spencer, N. D. *Langmuir* **2001**, *17*, 489−498.
(37) Ludtke, S. J.; He, K. E.; Heller, W. T.; Harroun, T. A.; Yang, L.; Huang, H. W. *Biochemistry* **1996**, *35*, 13723−13728.
(38) Kelly, S. T.; Zydney, A. L. *J. Membr. Sci.* **1995**, *107*, 115−127.
(39) Silin, V.; Weetall, H.; Vanderah, D. *J. Colloid Interface Sci.* **1997**, *185*, 94−103.
(40) Ojeda, J. J.; Romero-Gonzalez, M. E.; Pouran, H. M.; Banwart, S. A. *Mineral. Mag.* **2008**, *72*, 101−106.
(41) Jiang, W.; Saxena, A.; Song, B.; Ward, B. B.; Beveridge, T. J.; Myneni, S. C. B. *Langmuir* **2004**, *20*, 11433−11442.
(42) Heinrich, H. T. M.; Bremer, P. J.; Daughney, C. J.; McQuillan, A. J. *Langmuir* **2007**, *23*, 2731−2740.
(43) Calderon-Miranda, M. L.; Barbosa-Canovas, G. V.; Swanson, B. G. *Int. J. Food Microbiol.* **1999**, *51*, 31−38.
(44) Farkas, J.; Andrássy, E.; Mészáros, L.; Bánáti, D. *Acta Microbiol. Immunol. Hung.* **1995**, *42*, 19−28.
(45) Yuan, S.; Wan, D.; Liang, B.; Pehkonen, S. O.; Ting, Y. P.; Neoh, K. G.; Kang, E. T. *Langmuir* **2011**, *27*, 2761−2774.
(46) Malisova, B.; Tosatti, S.; Textor, M.; Gademann, K.; Zürcher, S. *Langmuir* **2010**, *26*, 4018−4026.
(47) Gao, G.; Yu, K.; Kindrachuk, J.; Brooks, D. E.; Hancock, R. E. W.; Kizhakkedathu, J. N. *Biomacromolecules* **2011**, *12*, 3715−3727.
(48) Glinel, K.; Jonas, A. M.; Jouenne, T.; Leprince, J.; Galas, L.; Huck, W. T. S. *Bioconj. Chem.* **2009**, *20*, 71−77.
(49) Park, K. D.; Kim, Y. S.; Han, D. K.; Kim, Y. H.; Lee, E.; Suh, H.; Choi, K. S. *Biomaterials* **1998**, *19*, 851−859.
(50) Timofeeva, L. M.; Kleshcheva, N. A.; Moroz, A. F.; Didenko, L. V. *Biomacromolecules* **2009**, *10*, 2976−2986.